

This discussion paper is/has been under review for the journal Biogeosciences (BG).  
Please refer to the corresponding final paper in BG if available.

# Comparative studies of pelagic microbial methane oxidation within two anoxic basins of the central Baltic Sea (Gotland Deep and Landsort Deep)

**G. Jakobs, G. Rehder, G. Jost, K. Kießlich, M. Labrenz, and O. Schmale**

Leibniz Institute for Baltic Sea Research Warnemünde (IOW), Rostock, Germany

Received: 3 July 2013 – Accepted: 13 July 2013 – Published: 20 July 2013

Correspondence to: G. Jakobs (gunnar.jakobs@io-warnemuende.de)

Published by Copernicus Publications on behalf of the European Geosciences Union.

**BGD**

10, 12251–12284, 2013

Comparative studies  
of pelagic microbial  
methane oxidation

G. Jakobs et al.

<a href="#">Title Page</a>	
<a href="#">Abstract</a>	<a href="#">Introduction</a>
<a href="#">Conclusions</a>	<a href="#">References</a>
<a href="#">Tables</a>	<a href="#">Figures</a>
<a href="#">◀</a>	<a href="#">▶</a>
<a href="#">◀</a>	<a href="#">▶</a>
<a href="#">Back</a>	<a href="#">Close</a>
<a href="#">Full Screen / Esc</a>	
<a href="#">Printer-friendly Version</a>	
<a href="#">Interactive Discussion</a>	

## Abstract

Pelagic methane oxidation was investigated in dependence on differing environmental conditions within the redox zone of the Gotland Deep (GD) and Landsort Deep (LD), central Baltic Sea. The redox zone of both deeps, which indicates the transition 5 between oxic and anoxic conditions, was characterized by a pronounced methane concentration gradient between the deep water (GD: 1233 nM, LD: 2935 nM) and the surface water (GD and LD < 10 nM), together with a  $^{13}\text{C}\text{CH}_4$  enrichment ( $\delta^{13}\text{C}\text{CH}_4$  deep water: GD  $-84\text{\textperthousand}$ , LD  $-71\text{\textperthousand}$ ; redox zone: GD  $-60\text{\textperthousand}$ , LD  $-20\text{\textperthousand}$ ;  $\delta^{13}\text{C}\text{CH}_4$  vs. Vienna Pee Dee Belemnite standard), clearly indicating microbial methane consumption 10 in that specific depth interval. Expression analysis of the methane monooxygenase identified one active type I methanotrophic bacterium in both redox zones. In contrast, the turnover of methane within the redox zones showed strong differences between the two basins (GD: max.  $0.12\text{ nM d}^{-1}$  and LD: max.  $0.61\text{ nM d}^{-1}$ ), with a four times 15 higher turnover rate constant ( $k$ ) in the LD (GD:  $0.0022\text{ d}^{-1}$ , LD:  $0.0079\text{ d}^{-1}$ ). Vertical mixing rates for both deeps were calculated on the base of the methane concentration profile and the consumption of methane in the redox zone (GD:  $2.5 \times 10^{-6}\text{ m}^2\text{s}^{-1}$ , LD:  $1.6 \times 10^{-5}\text{ m}^2\text{s}^{-1}$ ). Our study identified vertical transport of methane from the deep water body towards the redox zone as well as differing hydrographic conditions within the 20 oxic/anoxic transition zone of these deeps as major factors that determine the pelagic methane oxidation.

## 1 Introduction

Methane is an atmospheric trace gas that influences the climate and the atmospheric chemistry (Wuebbles and Hayhoe, 2002). It is generated in terrestrial, limnic and marine ecosystems by biotic and **abiotic mechanisms** (Segers, 1998; Reeburgh, 2007). 25 Although methane is trapped in aquatic sediments in vast amounts, marine environments only represent a negligible source for atmospheric methane (Reeburgh, 2007).

BGD

10, 12251–12284, 2013

## Comparative studies of pelagic microbial methane oxidation

G. Jakobs et al.

[Title Page](#)

[Abstract](#)

[Introduction](#)

[Conclusions](#)

[References](#)

[Tables](#)

[Figures](#)

◀

▶

◀

▶

[Back](#)

[Close](#)

[Full Screen / Esc](#)

[Printer-friendly Version](#)

[Interactive Discussion](#)



Comparative studies  
of pelagic microbial  
methane oxidation

G. Jakobs et al.

[Title Page](#)[Abstract](#)[Introduction](#)[Conclusions](#)[References](#)[Tables](#)[Figures](#)[◀](#)[▶](#)[◀](#)[▶](#)[Back](#)[Close](#)[Full Screen / Esc](#)[Printer-friendly Version](#)[Interactive Discussion](#)

The hydrographic situation of the Baltic Sea is characterized by a freshwater discharge from the rivers and episodic inflows of saline water from the North Sea (estuarine circulation) (Lass and Matthäus, 2008). The bottom topography of the Baltic Sea consists of a series of sub-basins that are separated by narrow sills, which hamper the continuous water exchange with the North Sea. Ventilation of the deep water by saline oxygenated water from the North Sea (so-called Major Baltic Inflows) occurred irregularly over the last decades leading to long periods of deep water stagnation in the central Baltic Sea (Matthäus et al., 2008; Reissmann et al., 2009); the last Major Baltic Inflow took place in year 2003. The more frequent but less intense inflows contain water masses with a density too low to displace the old stagnant water in the deep basins and propagate laterally into intermediate water layers of the central Baltic Sea (Matthäus et al., 2008).

In the central and southern Baltic Sea the less saline surface and more saline deep water cause the formation of a permanent density boundary, the halocline, which has a crucial effect on the vertical exchange of matter and the renewal of deep water (Reissmann et al., 2009). Especially the downward diffusion of oxygen is affected by this density boundary leading to a vertical biogeochemical zonation with oxygen-limiting conditions in the intermediate and deep water body and the turnover of organic matter by alternative microbial processes, like sulfate reduction (Lass and Matthäus, 2008). The oxygenated surface water and the anoxic deep water are separated by the redox zone. This zone is described as a smooth transition between oxic and anoxic conditions with an overlap of oxygen and hydrogen sulfide containing waters (Nausch et al., 2008; Labrenz et al., 2010). The pronounced chemical gradients in suboxic zones of stratified water columns are known to provide favorable conditions for different microbial processes such as ammonia oxidation, denitrification or methane oxidation (Brettar and Rheinheimer, 1992; Schubert et al., 2006a; Labrenz et al., 2010).

In the Gotland Basins, comprehensive water column investigations revealed a widespread release of methane from the sediments with strong methane enrichments in the stagnant anoxic water bodies (Gotland Deep and Landsort Deep; max. 504 nM

## Comparative studies of pelagic microbial methane oxidation

G. Jakobs et al.

[Title Page](#)[Abstract](#)[Introduction](#)[Conclusions](#)[References](#)[Tables](#)[Figures](#)[◀](#)[▶](#)[◀](#)[▶](#)[Back](#)[Close](#)[Full Screen / Esc](#)[Printer-friendly Version](#)[Interactive Discussion](#)

and 1086 nM, respectively; Schmale et al., 2010). Compared to the atmospheric equilibrium only slightly elevated methane concentrations prevail in the surface waters (Bange et al., 1994; Schmale et al., 2010; Gültzow et al., 2012). High resolution gas chemistry studies in the water column of the Gotland Basins showed a pronounced 5 methane gradient and an enrichment of  $^{13}\text{C}$   $\text{CH}_4$  within the pelagic redox zone that indicates microbial activity related to the aerobic oxidation of methane under suboxic conditions (Schnale et al., 2012). This finding is supported by earlier methane oxidation rate measurements indicating that methane is preferentially oxidized under low 10 oxygen concentrations (16 to 63  $\mu\text{M O}_2$ ) (Dzyuban et al., 1999). Schmale et al. (2012) also showed that aerobic methane oxidation within the pelagic redox zone of the Gotland Deep is performed by members of type I methanotrophic bacteria. Furthermore, 15 biomarker analysis could identify specific bacteriohopanepolyols (BHP) and phospholipid fatty acids (PLFA) that are characteristic for the presence of active type I methanotrophic bacteria (Berndmeyer et al., 2013) and these biomarkers were also used to record changes in the methanotrophic community throughout the Holocene (Blumberg et al., 2013).

Although microbial oxidation of methane in the water column represents an important sink of methane, the impact of dynamic environmental conditions like methane 20 source strength and hydrodynamic forces on the efficiency of that mechanism is still insufficiently described (Reeburgh, 2007; Schmale et al., 2012). With its distinct oxic and anoxic stratified zones that are episodically perturbed by oceanographic events, the Baltic Sea provides an ideal field to investigate these effects on the methane cycle. In this study we focus our work on the influence of different environmental and hydrographic conditions on the methane turnover within the pelagic redox zone. For this 25 scope, comparative interdisciplinary studies were carried out in the Gotland Deep and Landsort Deep. The combined data on methane chemistry, methane oxidation rates and molecular analysis will gain first insights into the temporal stability and regional transferability of microbial processes related to pelagic microbial methane consumption in the central Baltic Sea.

## 2 Study area

Investigations were carried out in the water column of the Gotland Deep (57°19.2' N 20°03.0' E, water depth 223 m) and Landsort Deep (58°35.0' N 18°14.0' E, water depth 422 m) located in the central Baltic Sea (Fig. 1). Both sampling sites are characterized by different basin structures and hydrographic conditions (see section through the central Baltic Sea, Fig. 1c). The Landsort Deep represents the deepest areal in the Western Gotland Basin (max. depth 460 m) with a relatively small spatial dimension. In contrast, the Eastern Gotland Basin represents the largest basin of the Baltic Sea with a maximum water depth of about 250 m at the Gotland Deep.

During an inflow of saline waters from the North Sea towards the central Baltic Sea, this water mass propagates first into the Eastern Gotland Basin. Depending on the strength of the inflow, the deep water mass can continue its path via a northern passage towards the Western Gotland Basin. The travel along different basins and sills promotes the mixing between saline bottom water and less saline overlying water masses, resulting in a decreasing salt content of the intruding water. Accordingly, the Landsort Deep is characterized by less frequent and weaker lateral intrusions, resulting in a more stable oxic/anoxic transition zone (redox zone) and a lower deep water salinity compared to the Gotland Deep (Matthäus et al., 2008).

## 3 Materials and methods

### 20 3.1 Sampling strategy

Samples were taken during cruise (06EZ/12/13) on R/V *Elisabeth Mann Borgese* in July/August 2012. Sampling procedures for molecular biological analysis and radio-tracer experiments were performed after first inspection of the physical parameters of the water column (e.g. salinity, turbidity) using a CTD probe (CTD system Seabird sbe911+ and a turbidity sensor ECO FLNTU, WET Labs) and methane concentration

[Title Page](#)[Abstract](#)[Introduction](#)[Conclusions](#)[References](#)[Tables](#)[Figures](#)[|◀](#)[▶|](#)[◀](#)[▶](#)[Back](#)[Close](#)[Full Screen / Esc](#)[Printer-friendly Version](#)[Interactive Discussion](#)

analysis on board to identify the most relevant depths intervals for methane oxidation. To obtain enough sample volume for all analysis water samples were taken within five casts on two consecutive days at each sampling site. Methane, oxygen and hydrogen sulfide analysis were performed on the first day of sampling. Water samples for determination of methane oxidation rates and molecular biological analysis were obtained on the following day. Between these two samplings the physical parameters of the water column showed no significant differences.

### 3.2 Gas analysis

#### 3.2.1 Methane, oxygen and hydrogen sulfide

For the determination of methane concentrations, water samples were transferred from the rosette water sampler into 250 mL glass flasks, and poisoned with 500  $\mu$ L saturated mercury chloride solution. Methane concentrations were determined directly after the cruise using a modified purge & trap procedure (Michaelis et al., 1990; Thomas, 2011). This modified method includes following process steps: the samples were stripped with helium to remove volatile constituents (purge step), dried using a Nafion® trap (Perma Pure LLC., USA), cryofocussed at  $-120^{\circ}\text{C}$  (ethanol/nitrogen) on HayeSep D® (Valco Instruments Company Inc., Switzerland) desorbed by heating at  $85^{\circ}\text{C}$ , and analyzed using a gas chromatograph (Shimadzu GC-2014) equipped with a flame ionization detector. The distribution of oxygen was determined by titration method (precision  $\pm 0.9 \mu\text{M O}_2$ ) and the hydrogen sulfide concentrations were measured calorimetrically according to the methylene blue method (precision  $\pm 1.0 \mu\text{M H}_2\text{S}$ ) (Grasshoff et al., 1999). Oxygen concentrations were only determined until first detection of hydrogen sulfide.

<a href="#">Title Page</a>	
<a href="#">Abstract</a>	<a href="#">Introduction</a>
<a href="#">Conclusions</a>	<a href="#">References</a>
<a href="#">Tables</a>	<a href="#">Figures</a>
<a href="#">◀◀</a>	<a href="#">▶▶</a>
<a href="#">◀</a>	<a href="#">▶</a>
<a href="#">Back</a>	<a href="#">Close</a>
<a href="#">Full Screen / Esc</a>	
<a href="#">Printer-friendly Version</a>	
<a href="#">Interactive Discussion</a>	

### 3.2.2 Stable carbon isotope ratio of methane

Gas samples for stable carbon isotope analysis of methane ( $\delta^{13}\text{C CH}_4$ ) were gained using a vacuum degassing system described in Keir et al. (2009) in detail. Following this method, a water sample of 600 mL was transferred into a 1100 mL pre-evacuated glass bottle leading to a partial degassing of the water sample. The extracted gas was decompressed to atmospheric pressure and subsequently transferred to a gastight burette. An aliquot of the extracted gas phase was conserved in a 10 mL pre-evacuated glass crimp vial containing a saturated sodium chloride solution poisoned with mercury chloride. The isotope ratio was determined using an isotope-ratio mass spectrometer (MAT 253, Thermo Electron, Germany) according to the method described by Schmale et al. (2012).  $\delta^{13}\text{C CH}_4$  values are expressed vs. VPDB (Vienna Pee Dee Belemnite) standard.

### 3.3 Methane oxidation rates

According to the sampling procedure by Reeburgh et al. (1991) water samples were directly transferred from the rosette sampler into transfusion bottles and sealed air-free with aluminum screw caps and natural rubber septa (Glasgerätebau Ochs Laborfachhandel e.K., Germany) to avoid any toxic effect from the sealing material. Three times the volume of the sample bottle (600 mL) was filled into the bottle in overflow, to avoid any entry of oxygen into the water samples. In addition, the sample bottles were flushed with argon before sampling. Each sample was labeled with a defined amount of radioactive methane ( $^{14}\text{CH}_4$  dissolved gas in sterile anoxic water, activity  $\approx 3\text{ kBq}$ , injection volume 100  $\mu\text{L}$ , preparation of the tracer was carried out according to Treude et al., 2005). In contrast to methods described by Reeburgh et al. (1991) and Durisch-Kaiser et al. (2005) a larger sample volume (600 mL) was chosen, to account for the low specific  $^{14}\text{CH}_4$  tracer activity used in this procedure and to obtain sufficient labeled oxidation products even in case of a low methane turnover. The accurate amount of  $^{14}\text{CH}_4$  activity that was added to the water samples was determined using the residual tracer

10, 12251–12284, 2013

BGD

Comparative studies  
of pelagic microbial  
methane oxidation

G. Jakobs et al.

[Title Page](#)

[Abstract](#)

[Introduction](#)

[Conclusions](#)

[References](#)

[Tables](#)

[Figures](#)

[◀](#)

[▶](#)

[◀](#)

[▶](#)

[Back](#)

[Close](#)

[Full Screen / Esc](#)

[Printer-friendly Version](#)

[Interactive Discussion](#)



Comparative studies  
of pelagic microbial  
methane oxidation

G. Jakobs et al.

[Title Page](#)[Abstract](#)[Introduction](#)[Conclusions](#)[References](#)[Tables](#)[Figures](#)[◀](#)[▶](#)[◀](#)[▶](#)[Back](#)[Close](#)[Full Screen / Esc](#)[Printer-friendly Version](#)[Interactive Discussion](#)

calculated according to Eq. (1),

$$r_{\text{ox}} = \frac{^{14}\text{CO}_2 \cdot \text{CH}_4}{^{14}\text{CH}_4 \cdot t \cdot 0.9} \left[ \text{nM d}^{-1} \right] \quad (1)$$

where  $^{14}\text{CO}_2$  is the radioactivity [dpm] of the microbial formed carbon dioxide,  $^{14}\text{CH}_4$  is the radioactivity [dpm] of the injected tracer,  $\text{CH}_4$  is the in situ methane concentration of the water sample [ $\text{nmol L}^{-1}$ ],  $t$  is the incubation time [d] and 0.9 the experimentally determined recovery factor (recovery factor of 1 indicates a quantitative release and capture of  $^{14}\text{CO}_2$  produced by the turnover of  $\text{CH}_4$ ). This factor was determined by a known amount of  $\text{H}^{14}\text{CO}_3^-$  dissolved in water, followed by acidification, and the capture of  $^{14}\text{CO}_2$  as described above. The turnover rate constant ( $k$ ) in Eq. (2) expresses the fraction of  $^{14}\text{CH}_4$  that is oxidized per unit time,

$$k = \frac{^{14}\text{CO}_2}{^{14}\text{CH}_4 \cdot t \cdot 0.9} \left[ \text{d}^{-1} \right] \quad (2)$$

Integrated methane oxidation rates ( $\text{ir}_{\text{ox}}$ ) over the depth interval of the redox zone were calculated by the trapezoid-rule according to Eq. (3), where  $\text{dz}$  [m] is the difference between two consecutive sampling depths,  $f(z)$  and  $f(z + \text{dz})$  are the corresponding oxidation rates ( $r_{\text{ox}}$ ) [ $\mu\text{mol d}^{-1} \text{m}^{-3}$ ].

$$\text{ir}_{\text{ox}} = \frac{1}{2} (f(z) + f(z + \text{dz})) \text{dz} \left[ \mu\text{mol d}^{-1} \text{m}^{-2} \right] \quad (3)$$

### 3.4 *pmoA* gene and transcript analysis

1000 mL of each sample were filtered on a Durapore filter (0.2  $\mu\text{m}$  pore size, GVWP, Merck Millipore, USA), frozen in liquid nitrogen and stored at  $-80^\circ\text{C}$ . DNA and RNA were extracted from frozen filters as described by Weinbauer et al. (2002). *pmoA* transcripts were analyzed with reverse transcriptase-PCR (30–33 cycles) using the primer

[Title Page](#)

[Abstract](#)

[Introduction](#)

[Conclusions](#)

[References](#)

[Tables](#)

[Figures](#)

[◀](#)

[▶](#)

[◀](#)

[▶](#)

[Back](#)

[Close](#)

[Full Screen / Esc](#)

[Printer-friendly Version](#)

[Interactive Discussion](#)



system A189f/mb661r (Holmes et al., 1995; Costello and Lidstrom, 1999) followed by DGGE fingerprinting as described in Schmale et al. (2012). Visible bands were cut out of the gel, reamplified and sequenced by LGC Genomics GmbH (Berlin, Germany). Sequences were checked for quality using SeqMan software (DNASTAR Inc., USA).

5 Phylogenetic affiliations of the partial sequences were initially estimated with the program BLAST (Altschul et al., 1990). In addition 50 ng DNA of each water sample was processed via PCR (30–35 cycles) and DGGE under the same conditions.

## 4 Results

### 4.1 Gotland Deep

10 During our field studies the temperature and salinity profiles (Fig. 2a) demonstrated strong vertical gradients, revealing thermohaline stratification with pronounced density differences of individual water bodies. The thermocline extended from 15 to 30 m water depth and the halocline was located in a depth interval from 60 to 80 m. The vertical turbidity profile showed different distinct peaks with two maxima, one in the surface 15 water and the other in around 127 m water depth. According to the content of oxygen ( $O_2$ , Fig. 2b), the water column can be separated into different depths intervals (Tyson and Pearson, 1991; Rabalais et al., 2010), an oxic zone from 0 to 81 m (349–9  $\mu M O_2$ ), a suboxic zone from 81 to 143 m (< 9  $\mu M O_2$ ) and an anoxic zone below 143 m with no detectable  $O_2$  concentrations. Hydrogen sulfide concentrations ( $H_2S$ , Fig. 2b) build-up 20 slightly between 93 and 127 m (3–17  $\mu M H_2S$ ) but show a stronger increase below that depth interval (max. 172  $\mu M H_2S$ ). The turbidity anomalies covered a depth interval of approx. 62 m (81–143 m), reflecting the suboxic zone (redox zone) and the subsequent transition to anoxic conditions (chemocline) (Kamyshny et al., 2013). For the Gotland Deep it is known that  $O_2$  and  $H_2S$  can co-occur at the oxic/anoxic interface (Labrenz et al., 2010). However, based on the fact that  $O_2$  concentrations were only measured 25 until first detection of  $H_2S$ , the co-occurrence of  $O_2$  and  $H_2S$  is not documented in

BGD

10, 12251–12284, 2013

Comparative studies  
of pelagic microbial  
methane oxidation

G. Jakobs et al.

[Title Page](#)

[Abstract](#)

[Introduction](#)

[Conclusions](#)

[References](#)

[Tables](#)

[Figures](#)

[◀](#)

[▶](#)

[◀](#)

[▶](#)

[Back](#)

[Close](#)

[Full Screen / Esc](#)

[Printer-friendly Version](#)

[Interactive Discussion](#)



Comparative studies  
of pelagic microbial  
methane oxidation

G. Jakobs et al.

Title Page

Abstract

Introduction

Conclusions

References

Tables

Figures

|◀

▶|

◀

▶|

Back

Close

Full Screen / Esc

Printer-friendly Version

Interactive Discussion



our dataset. Assuming that the suboxic water layer is mirrored by the depth interval of turbidity anomalies (Kamyshny et al., 2013) the redox zone is positioned between 81 m and 143 m water depth (Fig. 2b).

The methane profile (Fig. 2b) revealed concentrations lower than 10 nM CH<sub>4</sub> in the surface water. Below 80 m water depth, the methane concentration increased with increasing water depth with a methane maximum of 1233 nM CH<sub>4</sub> in the bottom water at 223 m water depth. The stable carbon isotope ratios in the deep water body are characterized by relatively low  $\delta^{13}\text{C CH}_4$  values (−84 ‰ at 223 m water depth) and a continuous enrichment of  $^{13}\text{C CH}_4$  towards the redox zone with strongly increasing  $\delta^{13}\text{C CH}_4$  values between 90 and 80 m water depth ( $\delta^{13}\text{C CH}_4$  from −67 ‰ to −45 ‰). Above the redox zone the isotopic ratio shifted back to more negative values ( $\delta^{13}\text{C CH}_4$  from −45 ‰ to −68 ‰) and showed values at the sea surface that are close to atmospheric  $\delta^{13}\text{C}$  ratios of methane (−47.6 ‰, <http://www.esrl.noaa.gov/gmd/dv/iadv/>) measured in the Baltic Sea.

Methane oxidation rates were measured in the oxic, suboxic and anoxic part of the water column. The major consumption of methane occurred in a depth interval between 80 and 130 m (Fig. 2c). The highest rate was measured within the redox zone (0.12 nM d<sup>−1</sup> at 90 m water depth) with a turnover rate constant (*k*) of 0.0022 d<sup>−1</sup>.

Expression of the *pmoA* gene was restricted to only one type I methanotroph in a depth interval from 85 to 125 m. Sequence analysis revealed a similarity of 100 % to an uncultured bacterium named Uncultured\_GotDeep\_pmoA1 (accession number KC188735), which was already detected earlier in the central Baltic Sea (Schmale et al., 2012). *pmoA* genes could not be detected.

## 4.2 Landsort Deep

Water column data from the Landsort Deep display thermohaline stratification similar to that observed in the Gotland Deep (Fig. 3a). The thermocline extended from 10 to 30 m water depth, and the halocline was located in a depth interval from 50 to 80 m.

**Comparative studies of pelagic microbial methane oxidation**

G. Jakobs et al.

[Title Page](#)[Abstract](#)[Introduction](#)[Conclusions](#)[References](#)[Tables](#)[Figures](#)[|◀](#)[▶|](#)[◀](#)[▶|](#)[Back](#)[Close](#)[Full Screen / Esc](#)[Printer-friendly Version](#)[Interactive Discussion](#)

Apart from the turbidity signal in the surface water, a pronounced signal was present in a depth interval between approx. 91 and 130 m (Fig. 3a). The oxic zone extended from 0 to 84 m (351–9  $\mu\text{M O}_2$ ; see classification Sect. 4.1 above). Again following the assumption, that turbidity anomalies can be used as an indicator for the depth interval of

5  $\text{O}_2/\text{H}_2\text{S}$  transition zone (Kamyshny et al., 2013), the redox zone is positioned between 84 and 130 m water depth (Fig. 3b).  $\text{H}_2\text{S}$  concentrations increased only slightly within the lower redox zone and remained relatively constant towards the sediment. The deep water revealed maximal  $\text{H}_2\text{S}$  concentrations of about 14  $\mu\text{M}$ .

The methane concentration profile showed a strong enrichment close to the bottom 10 (2935  $\mu\text{M CH}_4$  at 422 m), a pronounced methane gradient within the redox zone (from 80 to 124 m) and methane concentrations lower than 10 nM  $\text{CH}_4$  in the surface water. At the redox zone, a sharp isotopic shift was found between 99 and 85 m ( $\delta^{13}\text{C CH}_4$ , from  $-71\text{ ‰}$  to  $-20\text{ ‰}$  in the upper part of the redox zone).

Methane oxidation was detected throughout the water column, whereby the major 15 consumption of methane took place between 80 and 115 m water depth (Fig. 3c). The highest rate was measured within the redox zone ( $0.61\text{ nM d}^{-1}$  at 90 m water depth) with a turnover rate constant ( $k$ ) of  $0.0079\text{ d}^{-1}$ .

As determined for the Gotland Deep, the expression of the *pmoA* gene was restricted to the Uncultured GotDeep\_pmoA1 in a depth interval from 70 to 115 m (Fig. 3c). This 20 time, *pmoA* genes were detected between 80 and 115 m water depth.

## 5 Discussion

Our physical, chemical and microbiological results show considerable differences between both deeps. In the following chapter, we will discuss the different factors controlling the fate of methane in the Landsort Deep (LD) and Gotland Deep (GD) based on 25 data of the methane dynamics and the hydrodynamic situation.

### 5.1.1 Concentration and stable isotope pattern

Pelagic methane consumption is often reflected by the concentration distribution of methane and its stable carbon isotope pattern (Whiticar, 1999; Reeburgh, 2007; 5 Schmale et al., 2010). Our dataset points to prominent microbial methane consumption within the redox zones in both deeps (Figs. 2 and 3). The significance of this specific depth interval is emphasized by a constant methane concentration decrease and a pronounced change of the  $\delta^{13}\text{C CH}_4$  values. Here, the observed enrichment of  $^{13}\text{C CH}_4$  within the redox zone in both deeps can be explained by isotopic discrimination during 10 microbial methane oxidation due to the kinetic isotope effect that leads to an enrichment of  $^{13}\text{C CH}_4$  in the residual methane pool (Whiticar, 1999). In the LD, the steeper methane gradient together with the stronger  $^{13}\text{C CH}_4$  enrichment above the redox zone indicates more pronounced and efficient methane consumption compared to the GD assuming similar Eddy diffusion.

### 15 5.1.2 Methane oxidation rates

The outstanding position of the redox zone in the LD and GD as an important depth interval for microbial methane oxidation is also supported by measured elevated oxidation rates in this specific depth. However, remarkable differences are obvious between both deeps. Compared to the redox zone of the LD, which is characterized by the highest 20 oxidation rates (max. rate  $0.61 \text{ nM d}^{-1}$ ), the rates in the GD (max. rate  $0.12 \text{ nM d}^{-1}$ ) were much lower. Oxidation rates measured in the suboxic zone of the Black Sea are in the same order of magnitude as the data obtained in our study (rates range between  $1 \times 10^{-3}$  and  $1.6 \text{ nM d}^{-1}$ ) (Reeburgh et al., 1991; Durisch-Kaiser et al., 2005). Also the integrated oxidation rates calculated for the depth interval along the redox zone of the LD ( $4.85 \text{ } \mu\text{mol d}^{-1} \text{ m}^{-2}$ , 84–130 m) is almost three times as high as the integrated rate 25 in the GD ( $1.77 \text{ } \mu\text{mol d}^{-1} \text{ m}^{-2}$ , 81–143 m). At this zone the maximum turnover rate con-

stant ( $k$ ) detected in the LD ( $0.0079\text{ d}^{-1}$ ) is nearly four times as high as the constant in the GD ( $0.0022\text{ d}^{-1}$ , Fig. 4). Assuming that the turnover rate constant is reflecting the population size of methanotrophic microorganisms (Kessler et al., 2011), the growth of these organisms is maybe stimulated by the stronger stability of the intermediate water body that is less perturbed by lateral intrusions in the LD compared to the GD (see Sect. 5.2.2).

In addition to these perturbations, the concentration of methane also influences the abundance of the involved microbes within the redox zones in both deeps. Previous studies showed that increased substrate availability results in a dynamic adaption of the population size within the aerobic methanotrophic community (Valentine et al., 2001; Kessler et al., 2011). In conjunction with our studies, this would imply that in comparison to the GD the higher methane concentrations within the lower redox zone of the LD (GD:  $200\text{ nM CH}_4$  and LD:  $799\text{ nM CH}_4$ ) promote microbial methane oxidation and the growth of the methanotrophic community. The different population sizes within the redox zones are also supported by our DNA analysis. In contrast to the GD where no *pmoA* genes could be amplified in PCR reaction and thus probably were below the detection limit, DNA analysis for the identification of *pmoA* genes on the samples obtained in the LD yielded in positive PCR products.

To determine the kinetic fractionation factor ( $\alpha$ ) of microbial methane oxidation within the pelagic redox zones and further assess the methane oxidation in the pelagic chemocline, we created a plot of  $\delta^{13}\text{C CH}_4$  vs.  $1/\text{CH}_4$  (Fig. 5). To avoid any side effects in these calculations which could be caused by lateral intrusions, we used the dataset obtained in the LD in a first step. Motivated by the apparent restriction of methane oxidation within the redox zone, as observable from the methane concentration and isotope patterns in the LD (Fig. 3b), we applied a closed system Rayleigh fractionation approach (Coleman et al., 1981). The methane oxidation trend between the deep water ( $1192\text{ nM CH}_4$ ,  $\delta^{13}\text{C CH}_4$ :  $-71\text{ ‰}$ ) and the water depth which is characterized by the strongest  $^{13}\text{C CH}_4$  enrichment within the redox zone ( $\delta^{13}\text{C CH}_4$ :  $-20\text{ ‰}$  at  $85\text{ m}$  water depth) could be fitted best with a fractionation factor ( $\alpha$ ) of  $1.012$  (Fig. 5a). In a sec-

## Comparative studies of pelagic microbial methane oxidation

G. Jakobs et al.

[Title Page](#)[Abstract](#)[Introduction](#)[Conclusions](#)[References](#)[Tables](#)[Figures](#)[◀](#)[▶](#)[◀](#)[▶](#)[Back](#)[Close](#)[Full Screen / Esc](#)[Printer-friendly Version](#)[Interactive Discussion](#)

ond step, we used this derived  $\alpha$  to calculate the oxidation trend in the GD, which is characterized by a more disturbed intermediate water layer. The assumption of a similar  $\alpha$  is justified because of comparable temperatures and chemical conditions, and in particular by the identification of the same single methanotrophic bacterium identified in both deeps (see Sect. 5.1.3). The results, displayed in Fig. 5b, show that the entirely oxidation-controlled trend is not reflecting the natural conditions. The values obtained in the redox zone lie below the oxidation trend, which indicates that mixing is an additional factor controlling the methane dynamics in the Gotland Deep (Mau et al., 2012).

### 10 5.1.3 Aerobic methanotrophs in the redox zone

Sequence analysis revealed that in both deeps methane oxidation in the redox zone is restricted to type I methanotrophic bacteria indicating that the different environmental settings (i.e. methane concentrations and disturbances within the redox zone by lateral intrusions) did not fundamentally influence the microbial diversity of aerobic methanotrophs. The exclusive detection of type I methanotrophs is in good agreement with recently published biomarker analysis which confirm the absence of type II methanotrophic bacteria in the water column of the GD (Schmale et al., 2012; Berndmeyer et al., 2013). Our results are also in agreement with studies conducted by Schubert et al. (2006c) in the Black Sea, who identified type I methanotrophic bacteria as the most important methane consumer in the oxic/anoxic transition zone. However, other studies in the Black Sea also proved the existence of type II and X methanotrophs (Durisch-Kaiser et al., 2005; Blumenberg et al., 2007). The methanotrophic bacterium identified in the GD and LD is phylogenetically identical to the “Uncultured GotDeep\_pmoA1”, which was already detected earlier as the only methanotrophic phylotype in a Gotland Deep redox zone (Schmale et al., 2012). We interpret the restricted occurrence of only one active methanotrophic phylotype, in combination with a spatial and temporal structural stability, as a result of the lateral intrusions which can lead to an overlap of sulfide- and oxygen-containing waters at the Baltic Sea redox zones

<a href="#">Title Page</a>	
<a href="#">Abstract</a>	<a href="#">Introduction</a>
<a href="#">Conclusions</a>	<a href="#">References</a>
<a href="#">Tables</a>	<a href="#">Figures</a>
<a href="#">◀</a>	<a href="#">▶</a>
<a href="#">◀</a>	<a href="#">▶</a>
<a href="#">Back</a>	<a href="#">Close</a>
<a href="#">Full Screen / Esc</a>	
<a href="#">Printer-friendly Version</a>	
<a href="#">Interactive Discussion</a>	

(Labrenz et al., 2010; Dellwig et al., 2012). The toxicity of sulfide to many organisms may inhibit the activity of other methanotrophs than the detected phylotype. However, a higher diversity of active aerobic methanotrophic bacteria in the less disturbed redox zone of the LD could not be detected.

5 The detection of the *mcrA* gene for analyzing anaerobic methanotrophs was not performed in our studies due to the main focus on aerobic methane oxidation. From a theoretical point of view, sulfate-depending methane oxidation (AOM) in the anoxic water layer should be possible as the ambient sulfate concentrations (LD: 0.81 g kg<sup>-1</sup> and GD: 0.93 g kg<sup>-1</sup>; derived from the salinity profiles) would enable this process (Reeburgh, 10 2007). This assumption is supported by our methane oxidation rate measurements which indicate anaerobic turnover of methane in both basins. However, these oxidation rates are significantly affected by errors and cannot provide a clear evidence for the existence of AOM processes. The method developed for the present study was designed to analyze microbial methane oxidation within the oxic and suboxic part of the water 15 column, and the incubation time and the amount of <sup>14</sup>CH<sub>4</sub> tracer used were directed on this scientific focus.

## 5.2 Hydrodynamic controls on the fate of methane in the Gotland and Landsort Deep

### 5.2.1 Vertical mixing

20 The vertical transport of matter (e.g. nutrients, gases, particles) in the central Baltic Sea is strongly influenced by vertical mixing processes and the different intensities of mixing directly impact the concentration distribution pattern of chemical species in the water column (Nausch et al., 2008; Holtermann et al., 2012). Especially the transport across the chemocline is an important scientific subject as reduced and energy-rich 25 chemical species like CH<sub>4</sub>, H<sub>2</sub>S, iron (Fe<sup>2+</sup>) and manganese (Mn<sup>2+</sup>) are abundant in high concentrations within the deep water and can drive microbial reactions at the

BGD

10, 12251–12284, 2013

## Comparative studies of pelagic microbial methane oxidation

G. Jakobs et al.

[Title Page](#)

[Abstract](#)

[Introduction](#)

[Conclusions](#)

[References](#)

[Tables](#)

[Figures](#)

[|◀](#)

[▶|](#)

[◀](#)

[▶](#)

[Back](#)

[Close](#)

[Full Screen / Esc](#)

[Printer-friendly Version](#)

[Interactive Discussion](#)



oxic/anoxic transition zone (Labrenz et al., 2005; Dellwig et al., 2012; Schmale et al., 2012).

BGD

10, 12251–12284, 2013

5 Between 300 m water depth and the lower edge of the redox zone the LD is characterized by a uniform methane profile towards this zone whereas the **methane concentration** in the GD decrease constantly with decreasing depth. The same relationship is also reflected by the  $\text{H}_2\text{S}$  profiles and the  $\delta^{13}\text{C}\text{CH}_4$  distribution in the anoxic water bodies. This behavior may be related to enhanced vertical mixing processes via boundary effects above 300 m water depth in the LD that leads to a homogenization of the deep water body (Ledwell and Hickey, 1995; Axell, 1998).

10 Oceanographic studies by Axell (1998) show crucial differences in the vertical mixing rates ( $K_p$ : GD  $1.1 \times 10^{-5} \text{ m}^2 \text{s}^{-1}$ , LD  $6.2 \times 10^{-5} \text{ m}^2 \text{s}^{-1}$ , annual mean at 150 m water depth) of both deeps due to its differing topographic structure and the different position with respect to the coastline. The LD is well located within the coastal boundary layer (Fig. 1) and therefore influenced by high-energetic coastal processes leading to 15 a transfer of larger energy flux densities to the deep waters of the LD compare to the open sea situation of the GD (Axell, 1998). For the deep waters of the LD it is assumed that the coastal boundary layer leads to increasing mixing processes between 150–300 m water depths. Towards the bottom (below 300 m) the vertical mixing rates decrease strongly to values which are comparable with the ones determined for the deep 20 water of the GD. In the GD the deep water mixing is dominated by the energy input from the wind (Axell, 1998; Holtermann and Umlauf, 2012).

Another important factor that influences the deep water mixing in basins is the basin 25 geometry (hypsotherapy) and the resulting relation between the basin interior and the dimension of the basin boundary (BB). Near-boundary turbulence has a crucial impact on the basin-scale vertical mixing (Holtermann et al., 2012). Therefore, one can assume, that the relative small water volume (WV) of the LD and the relatively large surface of the BB (ratio WV/BB = 0.02) results in enhanced vertical mixing in the LD compared to the situation in the GD (WV/BB = 0.04).

[Title Page](#)

[Abstract](#)

[Introduction](#)

[Conclusions](#)

[References](#)

[Tables](#)

[Figures](#)

[◀](#)

[▶](#)

[◀](#)

[▶](#)

[Back](#)

[Close](#)

[Full Screen / Esc](#)

[Printer-friendly Version](#)

[Interactive Discussion](#)



Assuming that the flux of methane from the anoxic deep water to the redox zone and the consumption of methane within the redox zone are in steady state, we can use our dataset to calculate vertical mixing rates ( $K_p$ ) for the upper anoxic zone. Using the integrated methane oxidation rates ( $\text{ir}_{\text{ox}}$ ) in the redox zones (see Sect. 5.1.2) and the methane gradients within the upper anoxic zone,  $K_p$  can be calculated according to Eq. 5 (4), where  $c$  is the in situ concentration of methane [ $\mu\text{mol m}^{-3}$ ] and  $z$  the water depth [m].

$$K_p = \frac{\text{ir}_{\text{ox}}}{dc/dz} \left[ \text{m}^2 \text{d}^{-1} \right] \quad (4)$$

The mixing rates calculated by this method for the LD are one order of magnitude 10 higher than those for the GD (GD:  $2.5 \times 10^{-6} \text{ m}^2 \text{s}^{-1}$ , LD:  $1.6 \times 10^{-5} \text{ m}^2 \text{s}^{-1}$ ). This observed higher vertical mixing rate in the LD is in accordance with the observations of Axell (1998), who reported a 6 times larger  $K_p$  for the LD than for the GD at the 150 m depth level, though the absolute values are higher by a factor of 4. The enhanced vertical transport of methane implies a higher supply of substrate to the methanotrophic 15 community within the redox zone of the LD.

## 5.2.2 Lateral intrusions

The turbidity is often used as a marker to determine the depth of the chemocline. Turbidity anomalies near the chemocline reflect an incompletely understood phenomenon. It is often explained by the diffusion of reduced chemical species across the oxic–anoxic 20 interface, which lead to the precipitation of metal oxides (e.g. oxides of Fe and Mn) or the oxidation of  $\text{H}_2\text{S}$  to elemental sulfur ( $\text{S}^0$ ) (Dellwig et al., 2010; Kamyshny et al., 2013). Another theory is that the energy-rich compounds transported from the deep pool across the chemocline increase microbial turnover of matter and thus the abundance of bacteria in a discrete depth interval (Prokhorenko et al., 1994; Dellwig et al., 25 2010). However, the distribution pattern can also be used to discuss the stability of that

BGD

10, 12251–12284, 2013

Comparative studies  
of pelagic microbial  
methane oxidation

G. Jakobs et al.

[Title Page](#)  
[Abstract](#) [Introduction](#)  
[Conclusions](#) [References](#)  
[Tables](#) [Figures](#)  
[◀](#) [▶](#)  
[◀](#) [▶](#)  
[Back](#) [Close](#)  
[Full Screen / Esc](#)  
[Printer-friendly Version](#)  
[Interactive Discussion](#)



chemical boundary as lateral intrusions of external water masses into the oxic–anoxic interface will perturb the established chemical stratification (Kamyshny et al., 2013) and may inject O<sub>2</sub>/H<sub>2</sub>S enriched water into the suboxic zone (Dellwig et al., 2012). Our data shows that the turbidity profile of the GD (Fig. 2a) reveals different distinct peaks along the redox zone. Previous studies in the GD indicate, that these turbidity anomalies reflect the dynamic conditions within the redox zone (Lass et al., 2003; Dellwig et al., 2012). Therefore, lateral intrusions or internal waves produce perturbations in the intermediate water column and prevent the formation of a clearly defined suboxic zone. In contrast, the LD reveals only one pronounced turbidity signal with a constant decrease with increasing water depth (Fig. 3a). Even if this decrease can currently not be explained, the clear trend without turbidity spikes (in contrast to the observation in the GD) point to a more undisturbed situation in that transition zone (Dellwig et al., 2012; Kamyshny et al., 2013). Temperature-salinity diagrams (T-S) are useful approaches to identify the strength of intrusions in the central Baltic Sea (Dellwig et al., 2012). Signatures of intrusions can be identified in the GD by slight variations in the temperature and salinity profiles across the entire redox zone (see insert Fig. 6a). The LD is characterized by a relatively smooth T-S pattern indicating the undisturbed situation of this intermediate water layer (see insert Fig. 6b).

## 6 Conclusions

In the present study, methanotrophic processes within the stratified water columns of the Gotland Deep and Landsort Deep (central Baltic Sea) were investigated to reveal their dependence on different environmental settings. Within the pelagic redox zones of both deeps, microbial consumption of methane was identified by the distribution patterns of the concentration of methane, <sup>13</sup>C CH<sub>4</sub>, and elevated methane oxidation rates. In this intermediate depth interval one potentially active type I methanotrophic bacterium was identified at both sampling sites, indicating that the diverse hydrographic conditions have no influence on the composition of the methanotrophic community. In

contrast, the microbial turnover of methane in both deeps reveals considerable differences within the redox zones. The intensity of lateral intrusions and the vertical transport rate of methane from the deep methane pool into the redox zone are different between both deeps, and seem to represent the key-processes which control the turnover of methane within the oxic/anoxic transition zone. Our results confirm that pelagic microbial methane oxidation within redox gradients represent an efficient methane sink that prevents the escape of methane from the deep pool into the atmosphere. The comparative investigations in the Gotland Deep and Landsort Deep also indicate that this microbially mediated process can react on different environmental conditions by adapting the population size of methanotrophs and/or the rate of methane oxidation. Open questions regarding the involvement of other electron acceptors beside oxygen, the temporal dynamic of methane degradation as well as the verification of anaerobic methane oxidation in the deep anoxic waters need to be clarified in further studies.

**Acknowledgements.** Many thanks to the captain and the crew of R/V *Elisabeth Mann Borgese* for their support on cruise 06EZ/12/13. We would like to thank Tina Treude for the  $^{14}\text{CH}_4$  tracer preparation and for her support during the establishment of the labeling experiments at the IOW. We thank Iris Liskow for the technical assistance to install the combustion line and Stine Kedzior for sample measuring. We further thank Birgit Sadkowiak for oxygen and hydrogen sulfide analysis as well as Jan Donath for supplying bathymetric maps and CTD work. We gratefully acknowledge Peter Holtermann, Martin Blumberg, Christine Berndmeyer and Volker Thiel for fruitful discussions during paper preparation. This study was supported by the Deutsche Forschungsgemeinschaft (DFG) through the grant SCHM 2530/2-1.

## References

Altschul, S. F., Gish, W., Miller, W., Myers, E. W., and Lipman, D. J.: Basic local alignment search tool, *J. Mol. Biol.*, 215, 403–410, doi:10.1016/S0022-2836(05)80360-2, 1990.  
Axell, L. B.: On the variability of Baltic Sea deepwater mixing, *J. Geophys. Res.-Oceans*, 103, 21667–21682, 1998.

[Title Page](#)[Abstract](#)[Introduction](#)[Conclusions](#)[References](#)[Tables](#)[Figures](#)[|◀](#)[▶|](#)[◀](#)[▶](#)[Back](#)[Close](#)[Full Screen / Esc](#)[Printer-friendly Version](#)[Interactive Discussion](#)

Comparative studies  
of pelagic microbial  
methane oxidation

G. Jakobs et al.

<a href="#">Title Page</a>	
<a href="#">Abstract</a>	<a href="#">Introduction</a>
<a href="#">Conclusions</a>	<a href="#">References</a>
<a href="#">Tables</a>	<a href="#">Figures</a>
<a href="#">◀</a>	<a href="#">▶</a>
<a href="#">◀</a>	<a href="#">▶</a>
<a href="#">Back</a>	<a href="#">Close</a>
<a href="#">Full Screen / Esc</a>	
<a href="#">Printer-friendly Version</a>	
<a href="#">Interactive Discussion</a>	

Bange, H. W., Bartell, U. H., Rapsomanikis, S., and Andreae, M. O.: Methane in the Baltic and North Seas and a reassessment of the marine emission of methane, *Global Biogeochem. Cy.*, 8, 465–480, 1994.

Beal, E. J., House, C. H., and Orphan, V. J.: Manganese- and iron-dependent marine methane oxidation, *Science*, 325, 184–187, doi:10.1126/science.1169984, 2009.

Berndmeyer, C., Thiel, V., Schmale, O., and Blumenberg, M.: Biomarkers for aerobic methanotrophy in the water column of the stratified Gotland Deep (Baltic Sea), *Org. Geochem.*, 55, 103–111, doi:10.1016/j.orggeochem.2012.11.010, 2013.

Blumenberg, M., Seifert, R., and Michaelis, W.: Aerobic methanotrophy in the oxic-anoxic transition zone of the Black Sea water column, *Org. Geochem.*, 38, 84–91, doi:10.1016/j.orggeochem.2006.08.011, 2007.

Blumenberg, M., Berndmeyer, C., Moros, M., Muschalla, M., Schmale, O., and Thiel, V.: Bacteriohopanepolyols record stratification, nitrogen fixation and other biogeochemical perturbations in Holocene sediments of the central Baltic Sea, *Biogeosciences*, 10, 2725–2735, doi:10.5194/bg-10-2725-2013, 2013.

Boetius, A., Ravenschlag, K., Schubert, C. J., Rickert, D., Widdel, F., Gieseke, A., Amann, R., Joergensen, B. B., Witte, U., and Pfannkuche, O.: A marine microbial consortium apparently mediating anaerobic oxidation of methane, *Nature*, 407, 623–626, 2000.

Bourne, D. G., McDonald, I. R., and Murrell, J. C.: Comparison of *pmoA* PCR primer sets as tools for investigating methanotroph diversity in three danish soils, *Appl. Environ. Microbiol.*, 67, 3802–3809, 2001.

Brettar, I. and Rheinheimer, G.: Influence of carbon availability on denitrification in the central Baltic Sea, *Limnol. Oceanogr.*, 37, 1146–1163, 1992.

Coleman, D. D., Risatti, J. B., and Schoell, M.: Fractionation of carbon and hydrogen isotopes by methane-oxidizing bacteria, *Geochim. Cosmochim. Ac.*, 45, 1033–1037, doi:10.1016/0016-7037(81)90129-0, 1981.

Costello, A. M. and Lidstrom, M. E.: Molecular characterization of functional and phylogenetic genes from natural populations pf methanotrophs in lake sediments, *Appl. Environ. Microbiol.*, 65, 5066–5074, 1999.

Dellwig, O., Leipe, T., März, C., Glockzin, M., Pollehn, F., Schnetger, B., Yakushev, E. V., Böttcher, M. E., and Brumsack, H.-J.: A new particulate Mn-Fe-P-shuttle at the redoxcline of anoxic basins, *Geochim. Cosmochim. Ac.*, 74, 7100–7115, 2010.



Dellwig, O., Schnetger, B., Brumsack, H.-J., Grossart, H.-P., and Umlauf, L.: Dissolved reactive manganese at pelagic redoxclines (Part II): Hydrodynamic conditions for accumulation, *J. Marine Syst.*, 90, 31–41, 2012.

Durisch-Kaiser, E., Klauser, L., Wehrli, B., and Schubert, C.: Evidence of intense archaeal and bacterial methanotrophic activity in the Black Sea water column, *Appl. Environ. Microbiol.*, 71, 8099–8106, 2005.

Dzyuban, A. N., Krylova, I. N., and Kuznetsova, I. A.: Properties of bacteria distribution and gas regime within the water column of the Baltic Sea in winter, *Oceanology+*, 39, 348–351, 1999.

Ettwig, K. F., Butler, M. K., Le Paslier, D., Pelletier, E., Mangenot, S., Kuypers, M. M. M., Schreiber, F., Dutilh, B. E., Zedelius, J., de Beer, D., Gloerich, J., Wessels, H. J. C. T., van Alen, T., Luesken, F., Wu, M. L., van de Pas-Schoonen, K. T., Op den Camp, H. J. M., Janssen-Megens, E. M., Francoijis, K.-J., Stunnenberg, H., Weissenbach, J., Jetten, M. S. M., and Strous, M.: Nitrite-driven anaerobic methane oxidation by oxygenic bacteria, *Nature*, 464, 543–548, 2010.

Grasshoff, K., Ehrhardt, M., and Kremling, K.: *Methods of Seawater Analysis*, 3rd edn., Verlag Chemie, Gulf Publishing, Houston, 1999.

Güldzow, W., Rehder, G., Schneider v. Deimling, J., Seifert, T., and Tóth, Z.: One year of continuous measurements constraining methane emissions from the Baltic Sea to the atmosphere using a ship of opportunity, *Biogeosciences*, 10, 81–99, doi:10.5194/bg-10-81-2013, 2013.

Hallam, S. J., Grguis, P. R., Preston, C. M., Richardson, P. M., and DeLong, E. F.: Identification of methyl coenzyme m reductase A (mcrA) genes associated with methane-oxidizing archaea, *Appl. Environ. Microb.*, 69, 5483–5491, doi:10.1128/aem.69.9.5483-5491.2003, 2003.

Holmes, A. J., Costello, A., Lidstrom, M. E., and Murrell, J. C.: Evidence that particulate methane monooxygenase and ammonia monooxygenase may be evolutionarily related, *FEMS Microbiol. Lett.*, 132, 203–208, doi:10.1111/j.1574-6968.1995.tb07834.x, 1995.

Holtermann, P. L. and Umlauf, L.: The Baltic Sea Tracer Release Experiment: 2. mixing processes, *J. Geophys. Res.*, 117, C01022, doi:10.1029/2011jc007445, 2012.

Holtermann, P. L., Umlauf, L., Tanhua, T., Schmale, O., Rehder, G., and Waniek, J. J.: The Baltic Sea Tracer Release Experiment: 1. mixing rates, *J. Geophys. Res.*, 117, C01021, doi:10.1029/2011jc007439, 2012.

## Comparative studies of pelagic microbial methane oxidation

G. Jakobs et al.

[Title Page](#)[Abstract](#)[Introduction](#)[Conclusions](#)[References](#)[Tables](#)[Figures](#)[◀](#)[▶](#)[◀](#)[▶](#)[Back](#)[Close](#)[Full Screen / Esc](#)[Printer-friendly Version](#)[Interactive Discussion](#)

Kamyshny Jr., A., Yakushev, E. V., Jost, G., and Podymov, O. I.: Role of sulfide oxidation intermediates in the redox balance of the oxic–anoxic interface of the Gotland Deep, Baltic Sea, in: Chemical Structure of Pelagic Redox Interfaces, edited by: Yakushev, E. V., The Handbook of Environmental Chemistry, Springer, Berlin, Heidelberg, 95–119, 2013.

5 Keir, R., Schmale, O., Seifert, R., and Sütlenfuß, J.: Isotope fractionation and mixing in methane plumes from the Logatchev hydrothermal field, *Geochem. Geophys. Geosy.*, 10, Q05005, doi:10.1029/2009GC002403, 2009.

10 Kessler, J. D., Valentine, D. L., Redmond, M. C., Du, M., Chan, E. W., Mendes, S. D., Quiroz, E. W., Villanueva, C. J., Shusta, S. S., Werra, L. M., Yvon-Lewis, S. A., and Weber, T. C.: A persistent oxygen anomaly reveals the fate of spilled methane in the Deep Gulf of Mexico, *Science*, 331, 312–315, doi:10.1126/science.1199697, 2011.

Knittel, K. and Boetius, A.: Anaerobic oxidation of methane: progress with an unknown process, *Annu. Rev. Microbiol.*, 63, 311–334, 2009.

15 Labrenz, M., Jost, G., Pohl, C., Beckmann, S., Martens-Habbena, W., and Jürgens, K.: Impact of different in vitro electron donor/acceptor conditions on potential chemolithoautotrophic communities from marine pelagic redoxclines, *Appl. Environ. Microbiol.*, 71, 6664–6672, doi:10.1128/aem.71.11.6664-6672.2005, 2005.

20 Labrenz, M., Sintes, E., Toetzke, F., Zumsteg, A., Herndl, G. J., Seidler, M., and Jürgens, K.: Relevance of a crenarchaeotal subcluster related to *Candidatus Nitrosopumilus maritimus* to ammonia oxidation in the suboxic zone of the central Baltic Sea, *ISME J.*, 4, 1496–1508, 2010.

Lass, H. U. and Matthäus, W.: General oceanography of the Baltic Sea, in: State and Evolution of the Baltic Sea, 1952–2005, edited by: Feistel, R., Nausch, G., and Wasmund, N., John Wiley & Sons, Inc., New Jersey, 5–44, 2008.

25 Lass, H. U., Prandke, H., and Liljebladh, B.: Dissipation in the Baltic proper during winter stratification, *J. Geophys. Res.*, 108, 3187, doi:10.1029/2002jc001401, 2003.

Ledwell, J. R. and Hickey, B. M.: Evidence for enhanced boundary mixing in the Santa Monica Basin, *J. Geophys. Res.*, 100, 20665–20679, doi:10.1029/94JC01182, 1995.

30 Matthäus, W., Nehring, D., Feistel, R., Nausch, G., Mohrholz, V., and Lass, H. U.: The inflow of high saline water into the Baltic Sea, in: State and Evolution of the Baltic Sea, 1952–2005, edited by: Feistel, R., Nausch, G., and Wasmund, N., John Wiley & Sons, Inc., New Jersey, 265–310, 2008.

BGD

10, 12251–12284, 2013

Comparative studies  
of pelagic microbial  
methane oxidation

G. Jakobs et al.

[Title Page](#)

[Abstract](#)

[Introduction](#)

[Conclusions](#)

[References](#)

[Tables](#)

[Figures](#)

◀

▶

◀

▶

[Back](#)

[Close](#)

[Full Screen / Esc](#)

[Printer-friendly Version](#)

[Interactive Discussion](#)



Mau, S., Rehder, G., Sahling, H., Schleicher, T., and Linke, P.: Seepage of methane at Jaco Scar, a slide caused by seamount subduction offshore Costa Rica, *Int. J. Earth Sci. (Geol. Rundsch.)*, 1–15, doi:10.1007/s00531-012-0822-z, 2012.

5 McDonald, I. R., Bodrossy, L., Chen, Y., and Murrell, J. C.: Molecular ecology techniques for the study of aerobic methanotrophs, *Appl. Environ. Microbiol.*, 74, 1305–1315, doi:10.1128/aem.02233-07, 2008.

10 Michaelis, W., Gerhard, B., Jenisch, A., Ladage, S., Richnow, H. H., Seifert, R., and Stoffers, P.: Methane and  $^3\text{He}$  anomalies related to submarine intraplate volcanic activities, *Mitteilungen aus dem Geologisch-Paläontologischen Institut der Universität Hamburg*, 69, 117–127, 1990.

Modin, O., Fukushi, K., and Yamamoto, K.: Denitrification with methane as external carbon source, *Water Res.*, 41, 2726–2738, 2007.

15 Nausch, G., Nehring, D., and Nagel, K.: Nutrient concentrations, trends and their relation to eutrophication, in: *State and Evolution of the Baltic Sea, 1952–2005*, edited by: Feistel, R., Nausch, G., and Wasmund, N., John Wiley & Sons, Inc., New Jersey, 337–366, 2008.

Prokhortenko, Y. A., Krasheninnikov, B. N., Agafonov, E. A., and Basharin, V. A.: Experimental studies of the deep turbid layer in the Black Sea, *Phys. Oceanogr.*, 5, 133–139, 1994.

20 Rabalaïs, N. N., Díaz, R. J., Levin, L. A., Turner, R. E., Gilbert, D., and Zhang, J.: Dynamics and distribution of natural and human-caused hypoxia, *Biogeosciences*, 7, 585–619, doi:10.5194/bg-7-585-2010, 2010.

Reeburgh, W. S., Ward, B. B., Whalen, S. C., Sandbeck, K. A., Kilpatrick, K. A., and Kerkhof, L. J.: Black Sea methane geochemistry, *Deep-Sea Res.*, 38, 1189–1210, 1991.

Reeburgh, W. S.: Ocean methane biogeochemistry, *Chem. Rev.*, 107, 486–513, 2007.

25 Reissmann, J. H., Burchard, H., Feistel, R., Hagen, E., Lass, H. U., Mohrholz, V., Nausch, G., Umlauf, L., and Wieczorek, G.: Vertical mixing in the Baltic Sea and consequences for eutrophication – a review, *Progr. Oceanogr.*, 82, 47–80, 2009.

Schmale, O., Schneider von Deimling, J., Gützow, W., Nausch, G., Waniek, J. J., and Rehder, G.: Distribution of methane in the water column of the Baltic Sea, *Geophys. Res. Lett.*, 37, L12604, doi:10.1029/2010gl043115, 2010.

30 Schmale, O., Blumberg, M., Kießlich, K., Jakobs, G., Berndmeyer, C., Labrenz, M., Thiel, V., and Rehder, G.: Aerobic methanotrophy within the pelagic redox-zone of the Gotland Deep (central Baltic Sea), *Biogeosciences*, 9, 4969–4977, doi:10.5194/bg-9-4969-2012, 2012.

[Title Page](#)

[Abstract](#)

[Introduction](#)

[Conclusions](#)

[References](#)

[Tables](#)

[Figures](#)

[◀](#)

[▶](#)

[◀](#)

[▶](#)

[Back](#)

[Close](#)

[Full Screen / Esc](#)

[Printer-friendly Version](#)

[Interactive Discussion](#)



Schubert, C. J., Coolen, M. J. L., Neretin, L. N., Schippers, A., Abbas, B., Durisch-Kaiser, E., Wehrli, B., Hopmans, E. C., Sininghe Damsté, J. S., Wakeham, S., and Kuypers, M. M. M.: Aerobic and anaerobic methanotrophs in the Black Sea water column, *Environ. Microbiol.*, 8, 1844–1856, 2006a.

5 Schubert, C. J., Durisch-Kaiser, E., Holzner, C. P., Klauser, L., Wehrli, B., Schmale, O., Greinert, J., McGinnis, D., De Batist, M., and Kipfer, R.: Methanotrophic microbial communities associated with bubble plumes above gas seeps in the Black Sea, *Geochim. Geophys. Geosy.*, 7, Q04002, doi:10.1029/2005GC001049, 2006b.

10 Schubert, C. J., Durisch-Kaiser, E., Klauser, L., Vazquez, F., Wehrli, B., Holzner, C. P., Kipfer, R., Schmale, O., Greinert, J., and Kuypers, M. M. M.: Recent studies on sources and sinks of methane in the Black Sea, in: *Past and Present Water Column Anoxia*, IV. Earth and Environmental Sciences edn., edited by: Neretin, L. N., NATO Science Series, Springer, the Netherlands, 419–441, 2006c.

15 Segers, R.: Methane production and methane consumption: a review of processes underlying wetland methane fluxes, *Biogeochemistry*, 41, 23–51, doi:10.1023/A:1005929032764, 1998.

20 Thomas, S.: Vergleich und Optimierung analytischer Methoden zur Bestimmung des Methangehalts in Seewasser, Diplomarbeit, Universität Rostock, 2011.

Treude, T., Boetius, A., Knittel, K., Wallmann, K., and Barker Joergensen, B.: Anaerobic oxidation of methane above gas hydrates at Hydrate Ridge, NE Pacific Ocean, *Mar. Ecol.-Prog. Ser.*, 264, 1–14, 2003.

25 Treude, T., Krüger, M., Boetius, A., and Jørgensen, B. B.: Environmental control on anaerobic oxidation of methane in the gassy sediments of Eckernförde Bay (German Baltic), *Limnol. Oceanogr.*, 1771–1786, 2005.

Tyson, R. V. and Pearson, T. H.: Modern and ancient continental shelf anoxia: an overview, Geological Society, London, Special Publications, 58, 1–24, doi:10.1144/gsl.sp.1991.058.01.01, 1991.

30 Valentine, D. L. and Reeburgh, W. S.: New perspectives on anaerobic methane oxidation, *Environ. Microbiol.*, 2, 477–484, 2000.

Valentine, D. L., Blanton, D. C., Reeburgh, W. S., and Kastner, M.: Water column methane oxidation adjacent to an area of active hydrate dissociation, El River Basin, *Geochim. Cosmochim. Ac.*, 65, 2633–2640, 2001.

## Comparative studies of pelagic microbial methane oxidation

G. Jakobs et al.

[Title Page](#)

[Abstract](#)

[Introduction](#)

[Conclusions](#)

[References](#)

[Tables](#)

[Figures](#)

◀

▶

[Back](#)

[Close](#)

[Full Screen / Esc](#)

[Printer-friendly Version](#)

[Interactive Discussion](#)



Weinbauer, M. G., Fritz, I., Wenderoth, D. F., and Höfle, M. G.: Simultaneous extraction from bacterioplankton of total RNA and DNA suitable for quantitative structure and functional analyses. *Appl. Environ. Microbiol.*, 68, 1082–1084, 2002.

Whiticar, M. J.: Carbon and hydrogen isotope systematics of bacterial formation and oxidation of methane. *Chem. Geol.*, 161, 291–314, 1999.

Wuebbles, D. J. and Hayhoe, K.: Atmospheric methane and global change, *Earth-Sci. Rev.*, 57, 177–210. doi:10.1016/S0012-8252(01)00062-9, 2002.

# Comparative studies of pelagic microbial methane oxidation

G. Jakobs et al.

Parameter	Gotland Deep	Landsort Deep
depth interval of the redox zone	81–143 m	84–130 m
$\delta^{13}\text{C CH}_4$ (redox zone)	–60––79 ‰	–20––72 ‰
max. $\text{CH}_4$ conc. (bottom water)	1233 nM, 223 m	2935 nM, 422 m
$\delta^{13}\text{C CH}_4$ (bottom water)	–84 ‰, 223 m	–71 ‰, 422 m
max. methane oxidation rate ( $r_{\text{ox}}$ )	0.12 nM d <sup>–1</sup> , 90 m	0.61 nM d <sup>–1</sup> , 90 m
max. turnover rate constant ( $k$ )	0.0022 d <sup>–1</sup>	0.0079 d <sup>–1</sup>
<b>integrated methane oxidation rate (ir<sub>ox</sub>)</b>	1.77 $\mu\text{mol d}^{-1} \text{m}^{-2}$	4.85 $\mu\text{mol d}^{-1} \text{m}^{-2}$
vertical mixing rates ( $K_p$ , upper anoxic zone)	$2.5 \times 10^{-6} \text{ m}^2 \text{s}^{-1}$	$1.6 \times 10^{-5} \text{ m}^2 \text{s}^{-1}$
<i>pmoA</i> detection (DNA analysis)	not achieved	80–115 m
<i>pmoA</i> gene expression (mRNA analysis)	85–125 m	70–115 m

12278



Comparative studies  
of pelagic microbial  
methane oxidation

G. Jakobs et al.

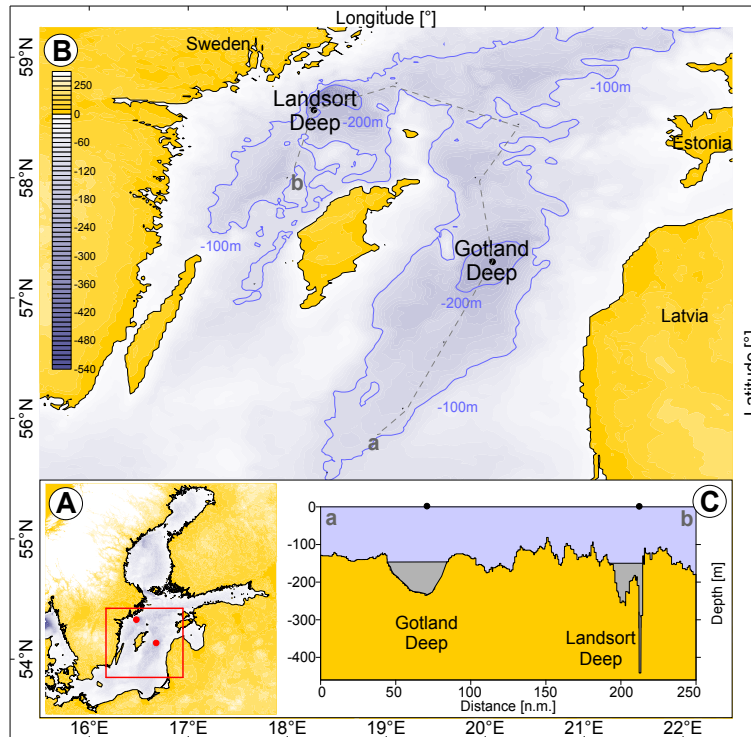


**Fig. 1.** (A) Sampling sites in the central Baltic Sea (red dots). (B) Bathymetric map of the central Baltic Sea with the Gotland Deep in the eastern and the Landsort Deep in the western Gotland Basin. (C) Cross section from the eastern to the western Gotland Basin. The grey shaded area below 150 m water depth was used for the calculation of the water volume/basin boundary ratio in Sect. 5.2.1 and illustrates the different spatial dimensions of the two sampling sites.

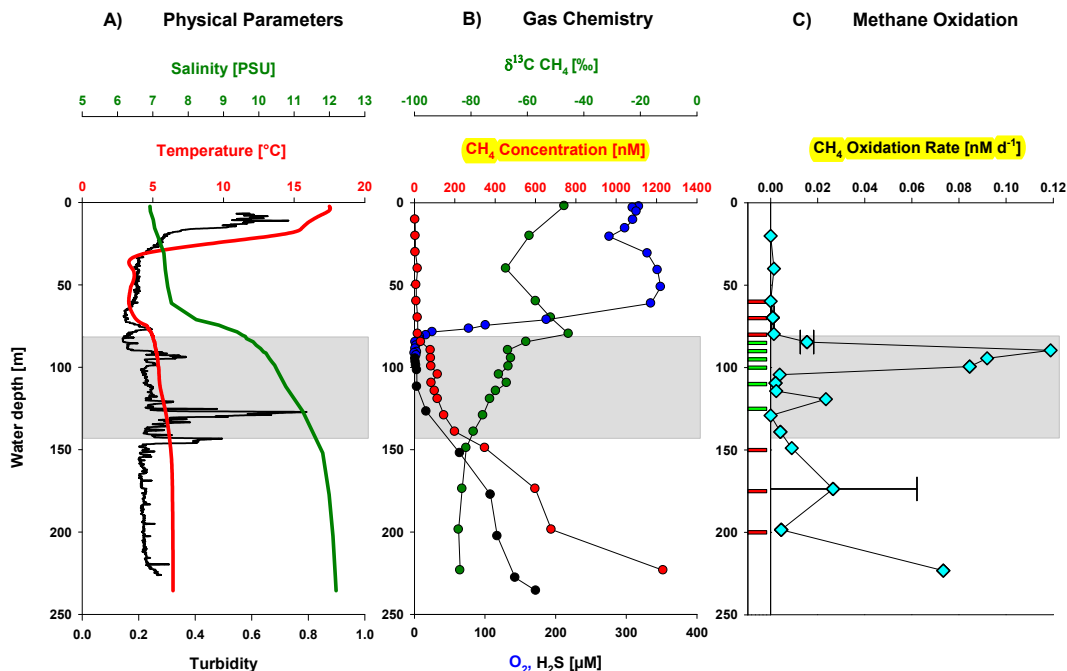


**Fig. 2.** Gotland Deep. **(A)** Vertical profiles of salinity (green), temperature (red), and turbidity (black); **(B)** oxygen (blue), hydrogen sulfide (black), methane (red), and  $\delta^{13}\text{C}$  values of methane (green); **(C)** methane oxidation rates (light blue), and sampling depths of *pmoA* gene expression analysis (green bars denote the occurrence and red bars the absence of active type I methanotrophs). The standard deviation ( $s$ ) for methane oxidation rates is indicated by error bars for the different water masses (oxic, suboxic and anoxic zone). The redox zone is indicated by the gray shaded area.

## Comparative studies of pelagic microbial methane oxidation

G. Jakobs et al.

[Title Page](#)

[Abstract](#)

[Introduction](#)

[Conclusions](#)

[References](#)

[Tables](#)

[Figures](#)

◀

▶

[Back](#)

[Close](#)

[Full Screen / Esc](#)

[Printer-friendly Version](#)

[Interactive Discussion](#)

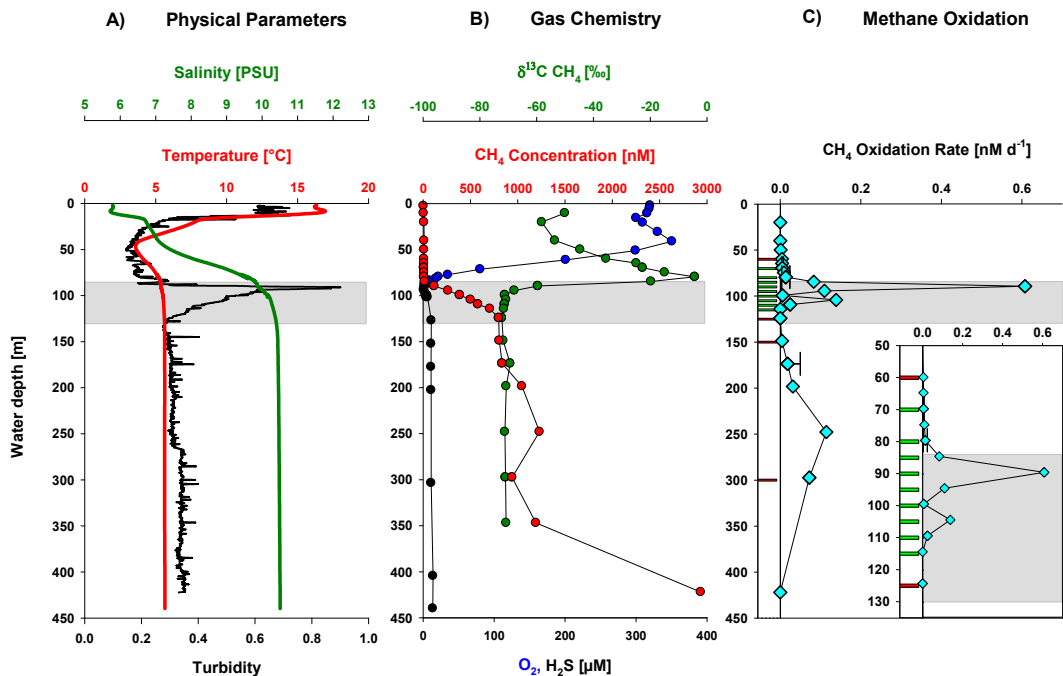


**Fig. 3.** Landsort Deep. **(A)** Vertical profiles of salinity (green), temperature (red), and turbidity (black); **(B)** oxygen (blue) and hydrogen sulfide (black), methane (red), and  $\delta^{13}\text{C}$  values of methane (green); **(C)** methane oxidation rates (light blue), and sampling depths of *pmoA* gene expression analysis (green bars denote the occurrence and red bars the absence of active type I methanotrophs). Error bars (standard deviation,  $s$ ) for the methane oxidation rates were determined for selected water depths within the oxic and anoxic water layer. The redox zone is indicated by the gray shaded area. The insert in **(C)** illustrates the depth interval of the redox zone in higher vertical resolution.

Title Page	
Abstract	Introduction
Inclusions	References
Tables	Figures
◀	▶
◀	▶
Back	Close
Full Screen / Esc	
Printer-friendly Version	
Interactive Discussion	

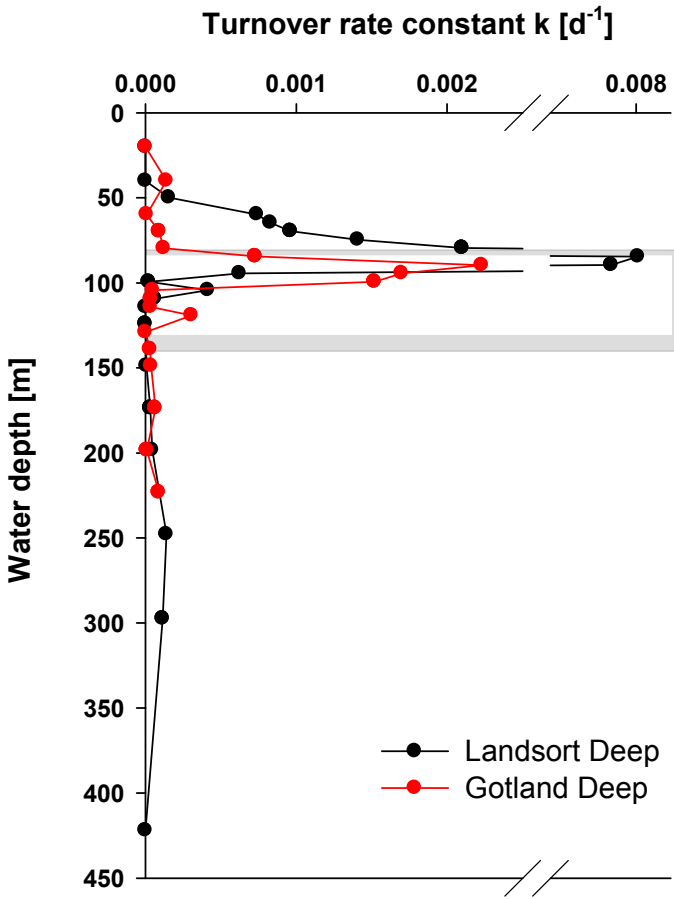


**Fig. 4.** Turnover rate constants ( $k$ ) from the Gotland Deep (red) and Landsort Deep (black). Indicated are the redox zones of the Gotland Deep (grey shaded area) and the Landsort Deep (white rectangle).

## Comparative studies of pelagic microbial methane oxidation

G. Jakobs et al.

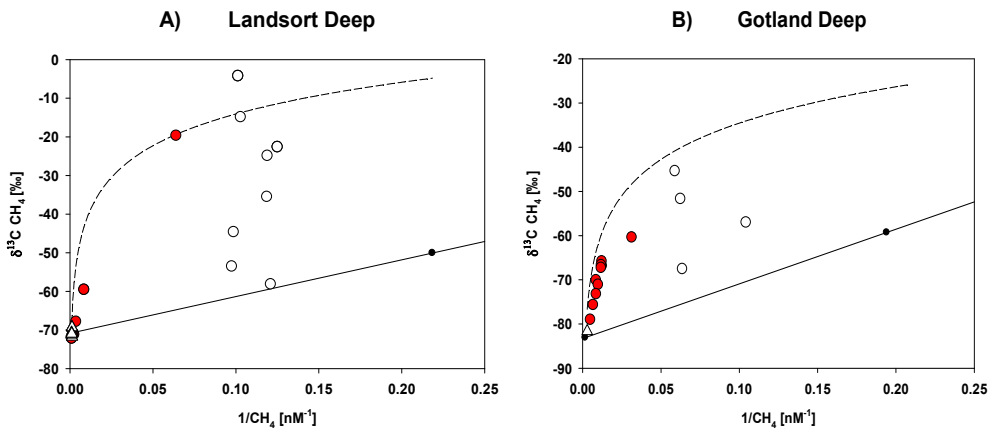


**Fig. 5.** Landsort Deep (**A**) and Gotland Deep (**B**).  $\delta^{13}\text{C CH}_4$  vs.  $1/\text{CH}_4$ . Please note different scales for  $\delta^{13}\text{C CH}_4$ . The solid lines denote mixing between deep and surface water, the dashed lines represent the oxidation trends based on a fractionation factor of  $\alpha = 1.012$ , the open triangles indicate the anoxic zone, the red circles the redox zone, and the open circles the oxic zone.

Title Page

## Abstract

## Introduction

## Conclusion

## References

## Tables

## Figures

1

1

Bad

Close

Full Screen / Esc

100% Biodegradable

## Discussion Paper | Comparative studies of pelagic microbial methane oxidation

G. Jakobs et al.

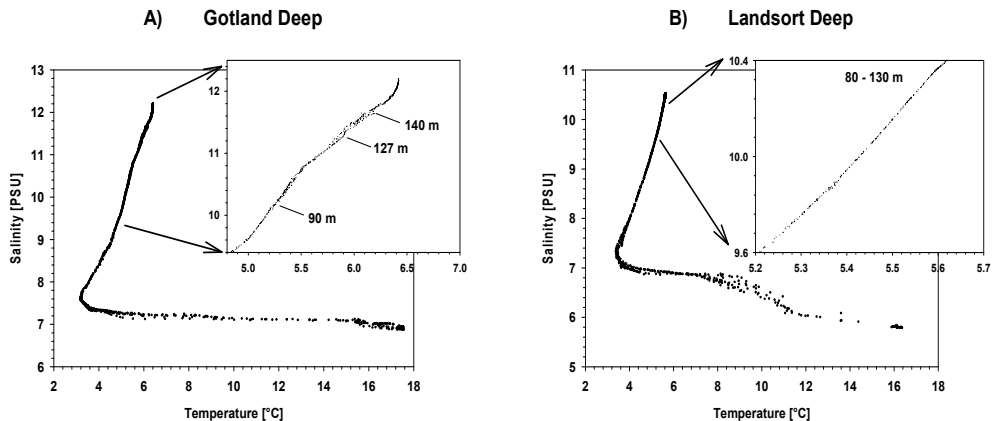


**Fig. 6.** Temperature-salinity diagrams. The inserts denote the depth interval where the redox zone is located.

[Title Page](#)

[Abstract](#) [Introduction](#)

[Conclusions](#) [References](#)

[Tables](#) [Figures](#)

[◀](#) [▶](#)

[◀](#) [▶](#)

[Back](#) [Close](#)

[Full Screen / Esc](#)

[Printer-friendly Version](#)

[Interactive Discussion](#)